JES
JOURNAL OF ENVIRONMENTAL SCIENCES
ISSN 1001-0742
CN 11-2629/X
February 1, 2013 Volume 25 Number 2
www.jesc.ac.cn

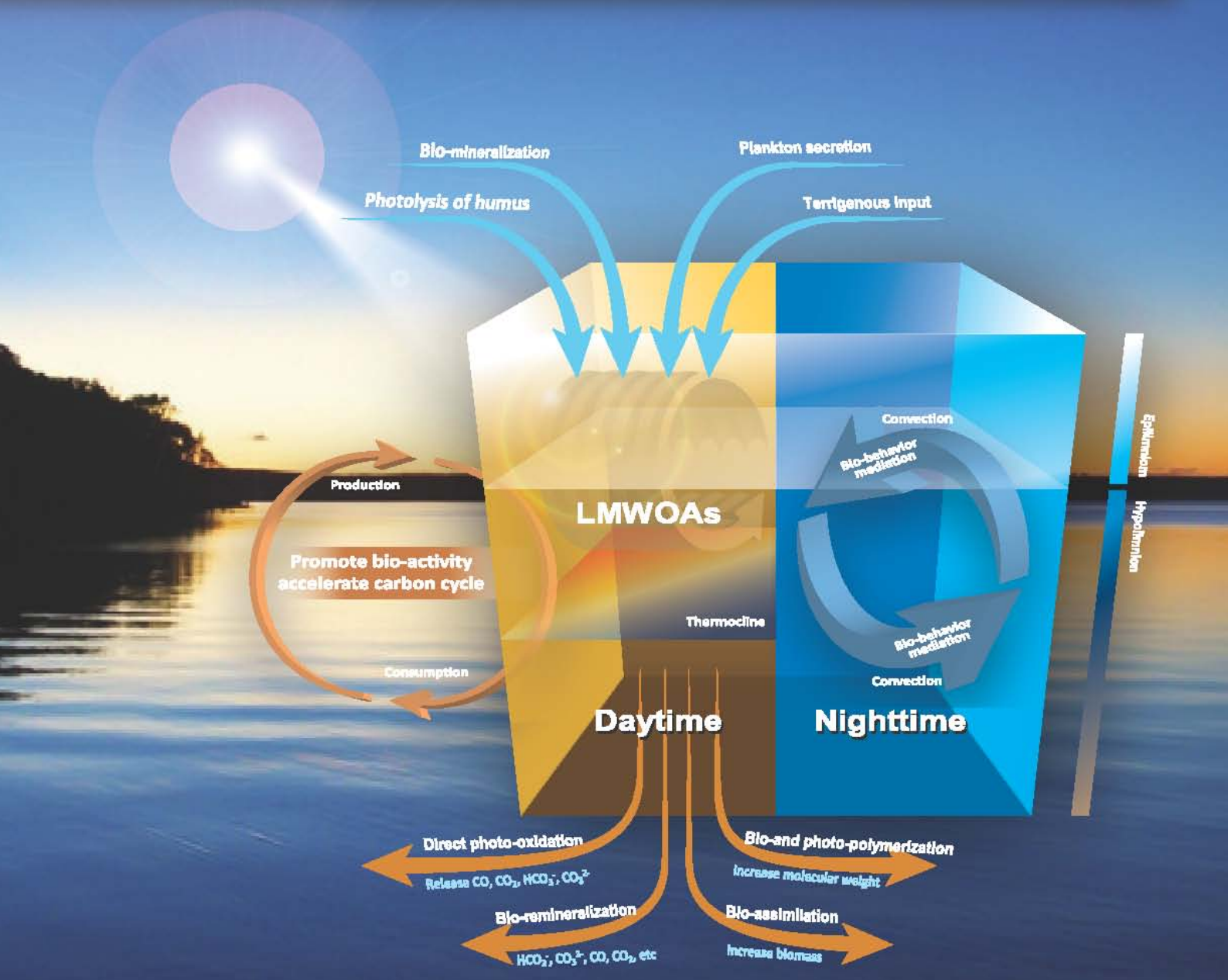

Science Press
Sponsored by
Research Center for Eco-Environmental Sciences
Chinese Academy of Sciences

ISSN 1001–0742 **Journal of Environmental Sciences** Vol. 25 No. 2 2013

CONTENTS

Serial parameter: CN 11-2629/X*1989*m*184*en*P*24*2013-2

Available online at www.sciencedirect.com
ScienceDirect
Journal of Environmental Sciences 2013, 25(2) 308–315
JOURNAL OF ENVIRONMENTAL SCIENCES
ISSN 1001-0742
CN 11-2629/X
www.jesc.ac.cn

Characterization of cake layer structure on the microfiltration membrane permeability by iron pre-coagulation

Jin Wang*, Siru Pan, Dongping Luo

Department of Municipal and Environmental Engineering, School of Civil Engineering, Beijing Jiaotong University, Beijing 100044, China

Received 12 March 2012; revised 28 August 2012; accepted 30 August 2012

Abstract

A cake layer is formed by coagulation aggregates under certain transmembrane pressure in the coagulation-microfiltration (MF) process. The characteristics of humic acid aggregates coagulated by different iron-based coagulants, such as charge, size, fractal dimension and compressibility, have an effect on the cake layer structure. At the optimum iron dose of 0.6 to 0.8 mmol/L for ferric chloride (FC) and polymer ferric sulfate (PFS) pre-coagulation, at the point of charge neutralization for near zero zeta potential, the aggregate particles produced possess the greatest size and highest fractal dimension, which contributes to the cake layer being most loose with high porosity and low compressibility. Thus the membrane filterability is better. At a low or high iron dose of FC and PFS, a high negative or positive zeta potential with high charge repulsion results in so many small aggregate particles and low fractal dimension that the cake layer is compact with low porosity and high compressibility. Therefore the membrane fouling is accelerated and MF permeability becomes worse. The variation of cake layer structure as measured by scanning electric microscopy corresponds with the fact that the smaller the coagulation flocs size and fractal dimension are, the lower the porosity and the tighter the cake layer conformation. This also explains the MF membrane flux variation visually and accurately.

Key words: coagulation-microfiltration process; cake layer structure; iron-based coagulant; zeta potential; porosity; scanning electric microscope

DOI: 10.1016/S1001-0742(12)60025-4

Introduction

Deterioration in the quality of source waters and increased demand coupled with more stringent water quality regulations have resulted in an increase in the implementation of pressure driven membrane technologies for purification of drinking water. Microfiltration (MF) and ultrafiltration (UF) are highly effective for turbidity, bacteria and protozoa removal, but achieve lower removal of natural organic matter (NOM), which is also a main factor in causing membrane fouling. Humic acid (HA) develops as the major component of NOM present in natural freshwater and therefore has been recognized as a significant generator of disinfection by-products (Park et al., 2002; Howe and Clark, 2006). HA consists of polycyclic aromatic macromolecules with a variety of oxygen-containing functional groups, and accounts for almost 50%–90% of the total organic matter in freshwater. A common method to reduce membrane fouling and improve filtered water quality simultaneously is to chemically coagulate the feed water prior to MF/UF (Chen et al., 2007; Choi and Dempsey, 2004).

Many previous investigations have suggested that optimizing pre-coagulation conditions can enhance the quality and quantity of the MF permeate through a coagulation-MF process (Choi and Dempsey, 2004; Kimura et al., 2008; Lee et al., 2000). Understanding the flocs' properties and the formation process of the cake layer on the membrane surface seem to be essential in controlling membrane fouling. Many factors related to the coagulation process, such as coagulation mechanisms which vary by species, concentration of coagulant and pH of the raw water, affect the floc characteristics, for example the size and fractal dimension, which play a significant role in inducing membrane fouling (Howe et al., 2006; Guigui et al., 2002). Aluminum salt coagulation conditions and their effect on membrane fouling have been studied carefully. For Al-based coagulation, the property of the flocs is dictated by the mechanism of coagulation induced by various hydrolyzed Al species (Lin et al., 2008). The enhancement of membrane permeability is strongly related to the strength and size distribution of the flocs (Wang et

* Corresponding author. E-mail: jwang1@bjtu.edu.cn

al., 2008, 2010; Lee et al., 2005). Lee et al. (2005) and Huang et al. (2011) have reported that strong flocs with compact structure as well as small size can form a cake layer of high permeability in membrane filtration.

However, the effect of iron coagulation on membrane fouling is not very clear. Moreover, the use of iron salts is increasing because iron is an essential element for the formation of hemoglobin, but aluminum is considered harmful to human organisms. Cheng and Chi (2002) compared the hydrolysis/coagulation behavior of polymeric and monomeric iron coagulants in HA solution and concluded that the formation of HA-$[Fe_m(OH)_x]_n^{(3m-x)n+}$ complexes and charge neutralization were responsible for HA removal. In the HA removal mechanism for poly ferric sulfate or chloride, it is believed that the complexation of HA with iron species by charge neutralization plays a more important role than HA adsorption on the iron hydroxide produced during hydrolysis (Cheng and Chi, 2002; Lei et al., 2009). Under the conditions of zero ionic strength and 25°C, the pK forms of the hydrolysis and solubility constants of iron hydroxide are 6 and 38 respectively (Duan and Gregory, 2003). Iron hydrolysis products with high positive charge exist at acidic pH, thus charge neutralization occurs predominantly. When the iron concentration is much above the solubility of iron hydroxide, the occurrence of sweep coagulation should also be considered.

The main objective of this study was to investigate the behavior of various monomer ferric chloride (FC) and polymer ferric sulfate (PFS) species as coagulants and their effects on HAs removal and membrane fouling when combined with the MF membrane process. The relationship of membrane permeability with cake layer conformation and coagulation aggregate structure is analyzed and described.

1 Materials and methods

1.1 Feed water

NOM in feed water was prepared using HA which was obtained from commercial sodium humate (Sigma-Aldrich, USA). Stock solutions were prepared by dissolving 1 g of powdered HA in 1 L of MilliQ water (>18 MΩ/cm). The HA concentration was evaluated with the ultraviolet absorbance measured at 254 nm (UV_{254}) using a UV-Vis Spectrophotometer (Varian-Cary 50 Bio, UK). The overall HA concentration was determined by comparing the absorbance and UV_{254} data with the appropriate calibration curves. The HA concentration of the synthetic raw water was diluted to 10 mg/L. Then 2 mmol/L sodium bicarbonate ($NaHCO_3$, Sigma-Aldrich, USA) was added to provide carbonate alkalinity similar to that of natural river water. The pH of the raw water was 7.7. Unless otherwise specified, all reagents and chemicals were of analytical grade.

1.2 Pre-coagulation microfiltration experiment

Two commercial iron-based coagulants, i.e., FC ($FeCl_3 \cdot 6H_2O$) and PFS (w (Fe) ≥ 18.5%, basicity: 10%) (Beijing Chemicals, China) were selected on account of their common use in water treatment plants. Stock solutions were prepared every day to achieve 0.1 mol/L calculated as the ferric ion concentration.

A dead-end batch MF unit was set up as shown in **Fig. 1**. MF membranes (hydrophilic, Millipore, USA) with a nominal pore size of 0.22 μm were used. The membrane material was a modified polyvinylidene fluoride. A fresh piece of membrane was used in every experiment. Prior to the filtration of the coagulation suspensions, MilliQ water was filtered through the fresh membrane in its non-fouled state until a steady permeate flux of 2.0 L/hr was observed. The effective MF membrane area was 28.26 cm^2. The

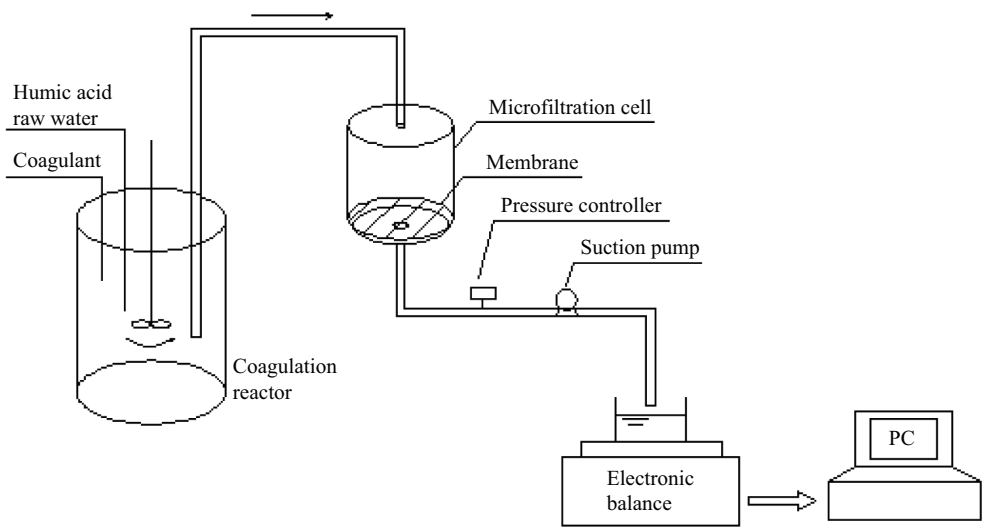

Fig. 1 Schematic diagram of the experimental set-up.

instantaneous mass of cumulative permeate was measured with an electronic balance (PB3002-SDR, Mettler Toledo Ltd., Switzerland) with automated data logging capability. The data were recorded from a connected PC at a predetermined time interval. The room temperature was maintained at 20°C.

In order to evaluate the pre-coagulation effect on membrane filterability, the same dose calculated as iron content was chosen for the two coagulants (0.2, 0.4, 0.6, 0.8 to 1.0 mmol/L). Coagulation was conducted in a 2.5-L cylindrical reactor under 1 min of rapid mixing (mean velocity gradient 100 sec^{-1}) and 20 min of flocculation (mean velocity gradient 25 sec^{-1}). Subsequently, the coagulation suspension was transferred from the coagulation reactor directly to a 0.23-L cylindrical filtration cell and filtered through a MF membrane under constant initial permeate flux. A weak stirring velocity was maintained in the reservoir to prevent flocs from settling. The MF membrane permeate was analyzed with UV_{254} for HA contents. Coagulation suspension samples were collected from the reactor to measure the zeta potential with a Zetasizer 3000HSa (Malvern Instruments, UK) and particle size with Malvern Mastersizer/E and obtain data for the fractal dimension calculation. The pH of the coagulated suspension was also measured, as shown in **Fig. 2**. The pH gradually decreased from 7.7 to 5.4 with iron addition increasing from 0.2 to 0.8 mmol/L no matter which iron compound was used, monomer FC or polymer PFS coagulant. When the dose increased further to 1.0 mmol/L, the monomer FC hydrolysis was more evident and pH value dropped faster to below 4.0 as the ferric ion hydrolysis exceeded the buffer capacity of the solution in comparison with PFS.

1.3 Flocs size distribution

A particle size analyzer (Mastersizer 2000, Malvern, UK), coupled with a small angle laser light scattering system, was used to observe the aggregation of particles and size distribution of flocs during coagulation. Floc size distribution and fractal dimension (d_F) were analyzed to determine the changes in floc characteristics under different HAs coagulation conditions. In this study the size distribution was determined using the polydisperse mode of analysis, and the mean diameter over the volume distribution was used to describe the mean particle size.

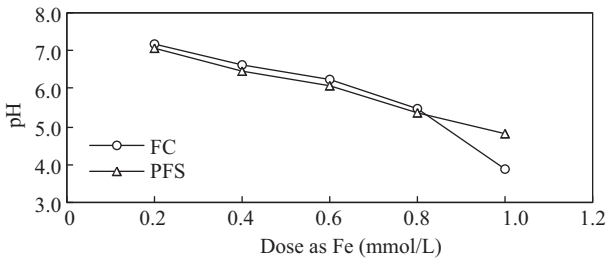

Fig. 2 pH variation of suspension coagulated by different iron-based coagulants and doses. FC: ferric chloride; PFS: polymer ferric sulfate.

Floc structure was represented as the fractal dimension. For colloidal aggregates, the cluster mass distribution can be presumed from the value of the mass fractal dimension, d_F. The d_F was calculated based on the small-angle static light scattering theory by graphing a log-log plot of intensity (I) vs. the wave number (Q). In order to calculate the fractal dimension from the log$I$–log$Q$ plot precisely, a Gaussian cutoff function was used to cover the Guinier regime data. The detailed relevant information has been discussed in previous work (Waite, 1999; Bushell and Amal, 2000).

Scanning electron micrographs (SEMs) of the membrane surfaces after filtration were obtained to visualize the foulant layers. The membranes were dried overnight in an oven at 60°C and observed under a field emission scanning electron microscope (LEO 1525, Carl Zeiss, Thornwood, USA) after sputter coating with a thin (10 nm) layer of gold.

2 Results and discussion

2.1 Variation of zeta potential

HAs are negatively charge due to the deprotonation of carboxylic and phenolic groups (Thurman and Malcolm, 1981). **Figure 3** shows the change in zeta potential of the HAs suspension with different ferric coagulants and doses. The charge neutralization point occurred between Fe doses of 0.6 to 0.8 mmol/L for both FC and PFS coagulants. However, for the monomer FC coagulant, significant charge reversion occurred as the zeta potential changed remarkably from –25 to 45 mV with increasing dosages from 0.2 to 1.0 mmol/L. A small change in the zeta potential to 8 mV was observed for the polymer coagulant PFS at iron dose enhanced to 1.0 mmol/L.

With iron dose increasing and pH decreasing, a different coagulation zone occurred, particularly at 1.0 mmol/L for FC, where the charge reversion and restabilization resulted in higher zeta potential. Colloidal particles are usually less negatively charged in the acidic pH range and over-adsorption of coagulant causes charge reversal on the surface, and thus the restabilization of the colloidal suspension at overdose. Liu and Chin (2009) also observed that

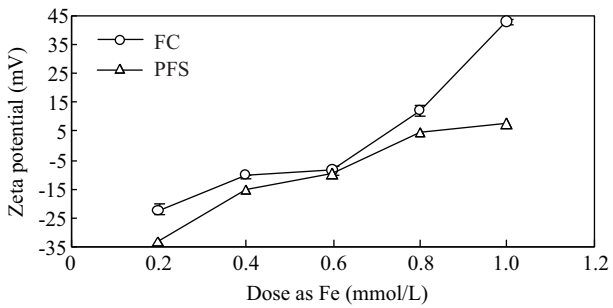

Fig. 3 The zeta potential of HAs suspension for different iron-based coagulants and doses.

restabilization did not occur when polymer iron chloride was used, whereas it occurred at acidic pH when $FeCl_3$ was used. The charge density of the polymers is less than the low molecular weight oligomeric species in $FeCl_3$ solution based on the charges each iron atom carries. The higher charge density of the oligomeric species may explain the restabilization observed in acidic conditions. When colloids are destabilized by polymeric coagulants in acidic pH, the lower charge density of the polymer makes the surface potential less positive than colloids destabilized by oligomeric species. Therefore, restabilization of colloids is then prevented as a result of coagulation by PFS.

2.2 Flocs size

Figure 4 shows the volume average diameter of flocs formed by FC and PFS coagulation for various dosages. The dissolved HA molecule is too small to be detected by the Malvern MasterSizer for the raw water sample without coagulation. There was a prominent indication of small flocs particularly in the size range 0.1–1 μm formed at the high iron dose of 1.0 mmol/L for FC pre-coagulation, which could be detrimental to MF performance as the particles had a relatively comparable size to the average membrane pore size 0.22 μm. At such a high dose, the HA molecule is covered by a large amount of ferric hydrolysis species with a high positive charge density, which makes it difficult for the particles to approach each other and achieve coagulation due to high electrostatic repulsion. Except at the 1.0 mmol/L ferric dose for FC pre-coagulation, the mean particle size was at a minimum and small particles with 1–10 μm were most prevalent at the low dose of 0.2 mmol/L, and the average particle size was at a maximum and small particles were least prevalent at the optimum dose of 0.6 mmol/L.

For PFS pre-coagulation, the small particles below 10 μm occurred mostly at the low 0.2 mmol/L ferric dose. At high 1.0 mmol/L doses, the particle size distribution was broad and presented double peaks, one between 1–10 μm and the other between 10–100 μm. The average particle size was the largest and small particles were least prevalent at dose 0.8 mmol/L, nearest the isoelectric point, as shown in **Fig. 3**. At either a low or high dose, the imbalance of electric charge reduced the efficiency of coagulation, which resulted in the generation of small flocs in the system.

The fractal dimensions d_F of HAs flocs formed under different iron doses by both FC and PFS are shown in **Fig. 5**, which were derived from the scattering patterns (Waite, 1999; Bushell and Amal, 2000). For both FC and PFS coagulation, the aggregate structure becomes compact because the zeta potential decreases and charge repulsion is reduced with ferric dose increasing from 0.2 to 0.6

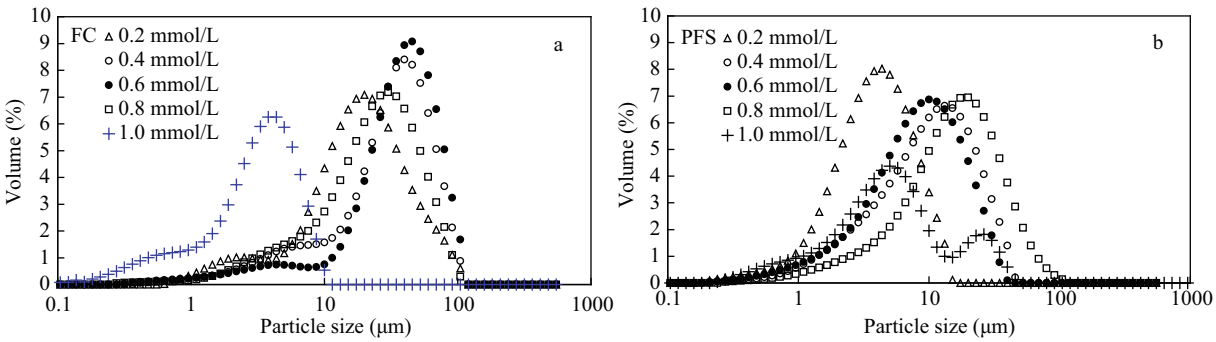

Fig. 4 Volume average diameter of flocs formed by FC and PFS coagulation for different iron doses. (a) FC pre-coagulation; (b) PFS pre-coagulation.

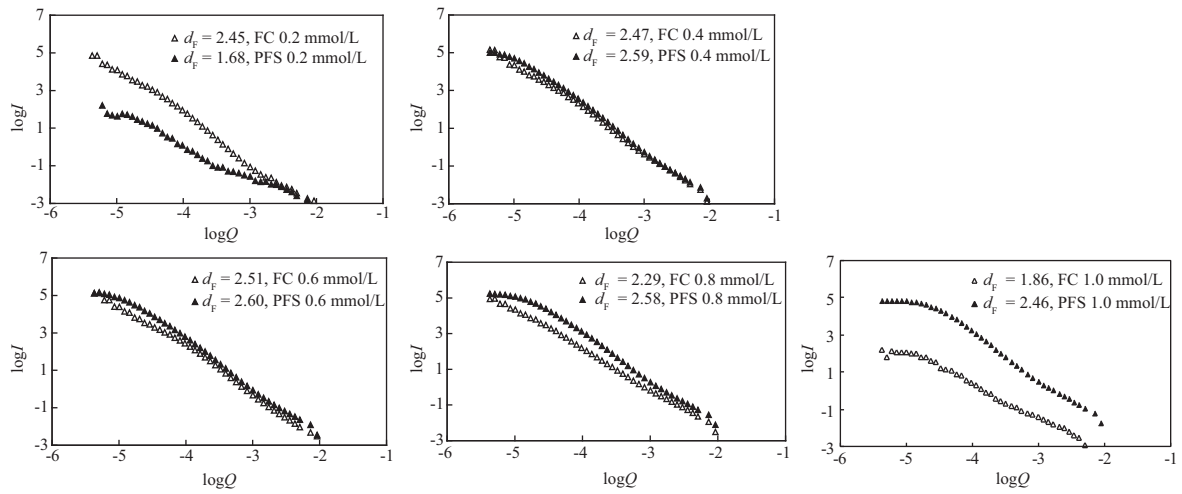

Fig. 5 Fractal dimensions (d_F) of flocs formed by FC and PFS coagulation with different iron doses. I: scattering light intensity; Q (nm^{-1}): wavenumber.

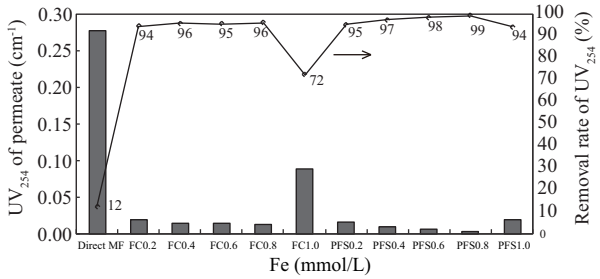

Fig. 6 HAs removal by MF with different iron-based coagulants and doses.

mmol/L. Whereas for ferric dose increasing continuously from 0.6 to 1.0 mmol/L, the aggregate structure became loose due to charge reversion and repulsion augmentation, in particular for FC coagulation. At the medium dose 0.4 to 0.8 mmol/L, the fractal dimension of flocs pre-coagulated by monomer FC was lower than with PFS, indicating that the aggregate structure pre-coagulated by monomeric FC was looser than that formed by polymeric PFS.

2.3 Removal of humic acid

Figure 6 shows the removal efficiency of HA, which is described by the surrogate parameter UV_{254} with different ferric coagulants and doses. Direct MF has almost no effect on HA removal because the size of the majority of HA is much smaller than the membrane pores. Within all the factors involved, what most affected the coagulation efficiency was pH and coagulant dose, which influenced the hydrolysis equilibrium of the coagulant species. At an iron dose of 1.0 mmol/L for FC pre-coagulation, the removal of HA by MF was only 72%, because so many particles smaller than 0.22 μm were formed as shown in **Fig. 4a**. The removal efficiency of HAs was 95% or even higher with ferric doses increasing from 0.4 to 0.8 mmol/L for both FC and PFS, indicating that effective coagulation pre-treatment formed large enough flocs and improved the interception efficiency of the MF membrane for HA removal. At the low dose of 0.2 mmol/L iron, the HA removal declined to 94% for FC and 95% for PFS, lower than that at the optimum dose. HA could not be coagulated well enough at such a low dose by either FC or PFS pre-coagulation.

2.4 Structure of cake layer on the membrane surface

Figure 7 shows the cake layer on the MF membrane surface scanned by SEM after typical precoagulation-MF experiments. The SEM photos visually illustrate the cake layer structure on the membrane surface, which is closely related with membrane filterability. In **Fig. 7**, compared to the layers formed at a low 0.2 mmol/L and high 1.0 mmol/L iron dose for both FC and PFS coagulation, the structure of the cake layer is more loose, porous and rough for the larger size and higher fractal dimension coagulation aggregates formed for the 0.6 mmol/L iron dose, as shown in **Figs. 4** and **5**, to resist the compressibility. However, the zeta potential was the most negative 35 mV at the minimum iron dose 0.2 mmol/L for PFS and the most positive 45 mV at the maximum dose 1.0 mmol/L for FC, so that the aggregate particles with the smallest size and lowest fractal dimension were occurred for great charge repulsion. Thus the cake layers were very compact and nearly no interstices shown as **Fig. 7b** and **e** for small particle size and large compressibility. Moreover, the cake layer was more porous coagulated by FC than PFS at the 0.2 mmol/L iron dose, but on the contrary the cake layer was looser by PFS than FC at the 1.0 mmol/L dose in **Fig. 7**, which was also consist with the comparison of the particle size and compressible strength. In general, the variation seen in the SEM photos corresponds completely with the fact that the smaller the coagulation flocs size and fractal dimension are, the tighter the cake layer conformation. However, the SEM photos give us the qualitative but hardly quantitative comparison completely.

Although the fractal dimension of the aggregates is higher for the medium iron dose of 0.6 mmol/L than for any other dose (**Fig. 5**), indicating more compact aggregates, the cake layer seen from SEM photos, on the contrary, is looser. The structure of the coagulation aggregates and the cake layer on the membrane surface are interrelated yet different. The structure of the cake layer is related to not only the aggregate fractal dimension but also aggregate size and compressibility. The coagulation particles were smaller due to higher charge repulsion at the low iron dose of 0.2 mmol/L for FC and PFS coagulants and at the high dose 1.0 mmol/L for FC (**Fig. 4**), producing a tight arrangement and low porosity in the cake layer; at the same time, the lower fractal dimension of flocs (**Fig. 5**) appears to result in more compressibility at a given transmembrane pressure, which also finally reduces the porosity of the cake layer. Therefore, the cake layer becomes more compact and tighter at lower and higher doses than at medium dose. In the end, the porosity of the cake layer formed through particle deposition plays the most important role in the filtration performance of low-pressure membranes.

2.5 Membrane filtration

The change in permeate flux during MF of raw water and suspensions pre-coagulated by FC and PFS coagulants with different ferric dosages is shown in **Fig. 8**. As the size of non-coagulated HAs is significantly smaller than the average membrane pore size, HAs removal was low for raw water, and thus the permeate flux only decreased slightly, which did not cause severe membrane fouling. SEM photos illustrate the cake layer fouling on the membrane surface visually, which is closely related with membrane filterability. The decline in permeate flux was slow and membrane fouling was alleviated for pre-coagulation with ferric doses of 0.6 and 0.8 mmol/L for both FC and PFS coagulants, where aggregate particles had greater size and

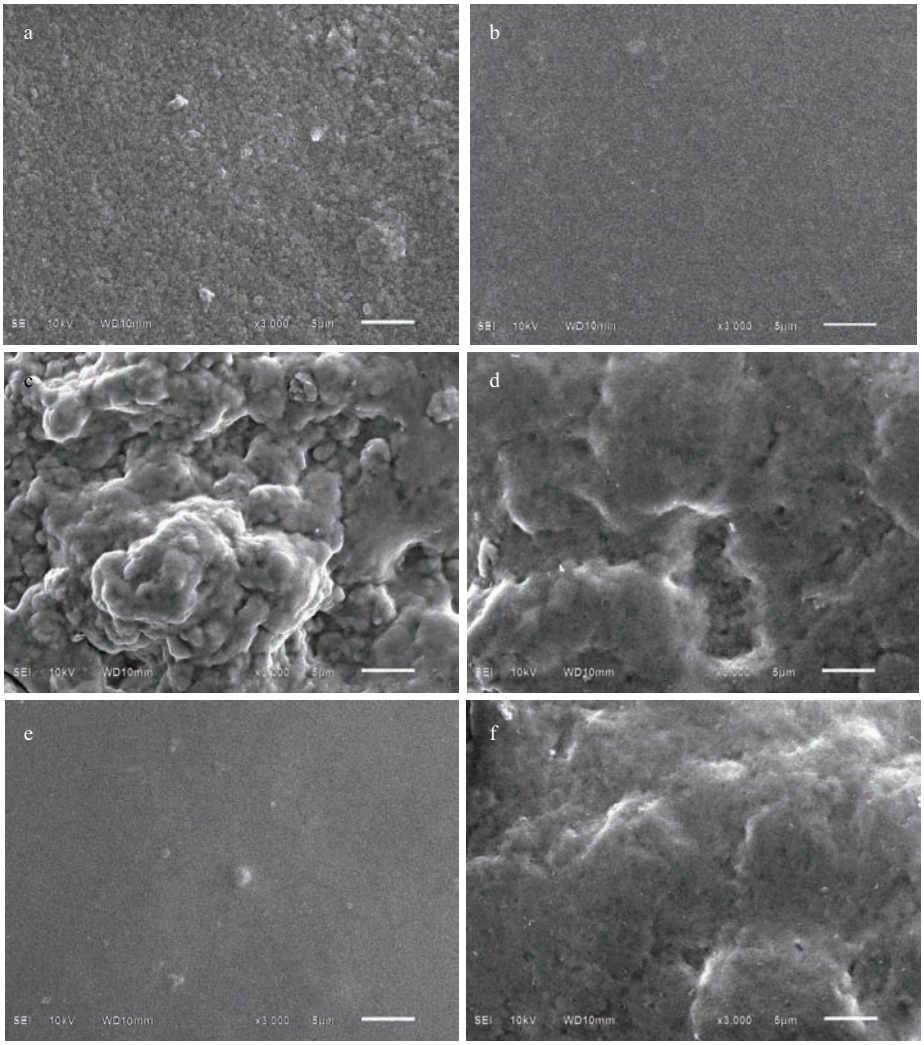

Fig. 7 SEM photos of cake layers on the membrane surface for different iron-based coagulants and doses: (a) FC 0.2 mmol/L; (b) PFS 0.2 mmol/L; (c) FC 0.6 mmol/L; (d) PFS 0.6 mmol/L; (e) FC 1.0 mmol/L; (f) PFS 1.0 mmol/L.

incompressible dimension, thus the cake layer was also loose as shown in **Fig. 7**. Barbot et al. (2008) also suggested that the optimal pre-coagulation condition for the coagulation/membrane filtration process is the formation of large flocs with a strong structure. Strong flocs can resist the stress of fluid during filtration, which facilitates the flow between aggregates within the cake.

The most drastic permeate flux decline occurred in the case of ferric overdosing (1.0 mmol/L) for FC pre-coagulation and underdosing (0.2 mmol/L) for both FC and PFS, in comparison with the optimum doses (0.6–0.8 mmol/L). When the ferric dose is either too high or too low, particle aggregation is not complete as a result of greater repulsion forces caused by high charge imbalances. Hence, the existing small particles and low porosity for compressibility produced a tighter cake layer and worsened MF membrane permeability.

It is noteworthy that the initial permeate flux (initial 10–15 min) for pre-coagulation by FC or PFS at the optimum dose of 0.6 and 0.8 mmol/L iron was even higher than that for direct MF, because the cake layer as a dynamic "membrane" forms quickly from large aggregates, which effectively restrains the fraction of smaller particles from severely fouling the MF membrane.

The volume average diameter and fractal dimension of coagulation flocs was measured to indicate the initial aggregates' size and structural characters of compactness and compressibility without MF, as shown in **Figs. 4** and **5**. With the MF process, the cake layer formed by the aggregates deposited on the membrane surface under a given pressure. When the fractal dimension of aggregates is lower, the higher compressibility results in smaller porosity in the cake layer. The smaller size and lower porosity produce higher cake layer specific resistance according to the Carman-Kozeny relationship:

$$\alpha = \frac{180(1-\varepsilon)}{\rho d^2 \varepsilon^3}$$

where, α (m/kg) is specific cake resistance; d (m) is particle diameter; ρ (kg/m^3) is suspension density; ε is the porosity of cake layer.

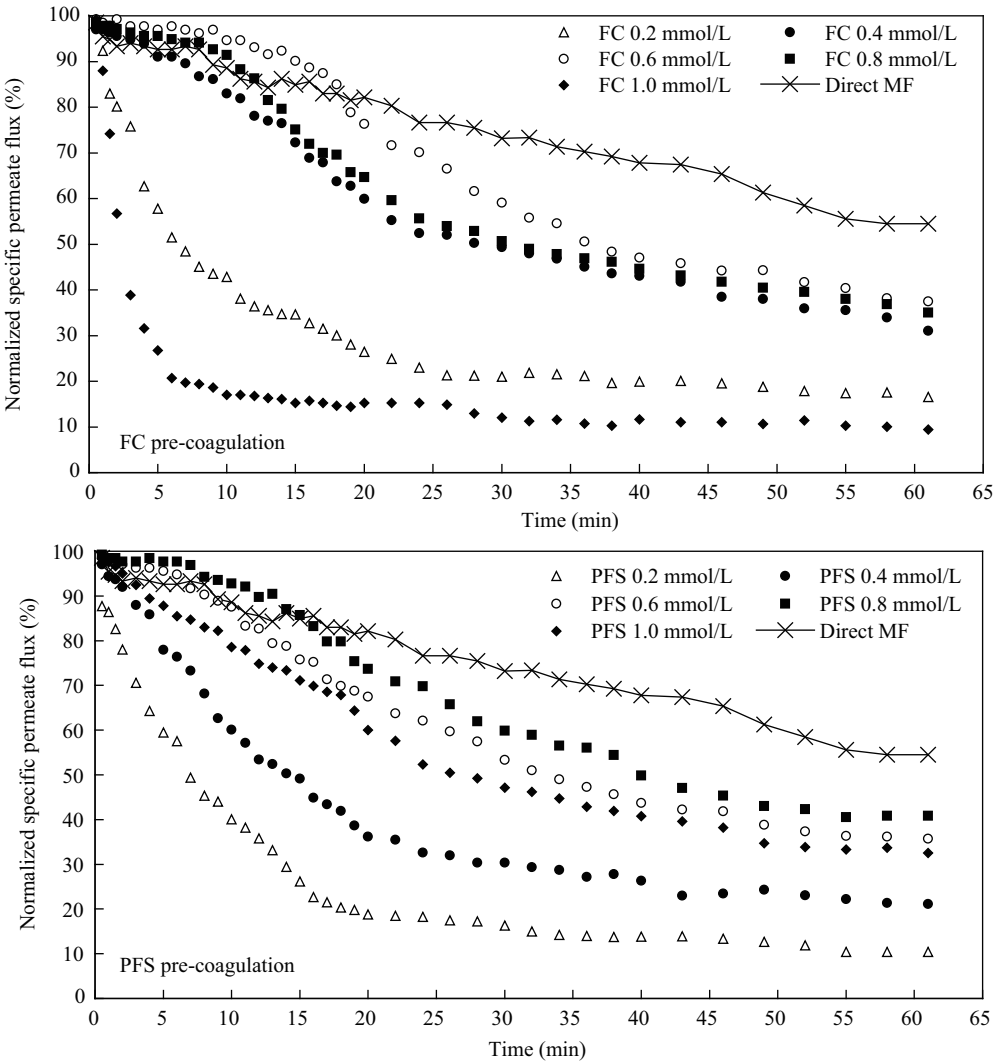

Fig. 8 Variation of membrane flux for different iron-based coagulants and doses.

The SEM photos in **Fig. 7** which showed the final cake layer structure on the membrane surface after MF verified the above deduction. Monitoring of the cake layer's formation and variation of the structure on-line could not be achieved without disturbing it. However, we can optimize the coagulation conditions to improve membrane filterability by analyzing the coagulation flocs' characters of charge, size, fractal dimension initially and the structure variation of the cake layer under the pressure of MF finally.

3 Conclusions

A cake layer is formed by coagulation aggregates under the influence of transmembrane pressure. The characteristics of aggregates pre-coagulated by iron-based coagulants, such as charge, size, fractal dimension and cake layer conformation, could have a major impact on the removal efficiency of HAs and the reduction of membrane fouling. The cake layer structure is related to aggregate structure but is not exactly the same because of compressibility. The structure of the cake layer on the membrane surface in the coagulation-MF process directly affects membrane fouling.

At the optimal dose of 0.6 to 0.8 mmol/L iron for FC or PFS precoagulation, the charge repulsion is at the lowest for near zero zeta potential, which results in larger coagulation particles and higher fractal dimension, and at the same time the cake layer is most loose with low compressibility and high porosity. Thus the membrane fouling is alleviated and MF filterability is better. At a low or high dose of FC or PFS, the high charge repulsion for high negative or positive zeta potential produces small aggregates but a low fractal dimension, so the cake layer is compact with high compressibility and low porosity. Therefore the membrane fouling is accelerated and MF permeability is worse.

The cake layer structure observed by SEM explains the MF membrane flux variation clearly. SEM photos show that the cake porosity is the most important factor affecting the hydraulic resistance of the cake layer. The

exploration of the relationship between floc properties and the corresponding cake layer properties indicates that the higher fractal dimension of stronger flocs with lower compressibility and larger size results in higher membrane flux in the coagulation-MF process.

Acknowledgments

This work was supported by the National Natural Science Foundation of China (No. 50978014) and the Fundamental Research Funds for the Central Universities (No. 2011JBM077).

References

Barbot E, Moustier S, Bottero J Y, Moulin P, 2008. Coagulation ultrafiltration: understanding of the key parameters of the hybrid process. *Journal of Membrane Science*, 325(2): 520–527.

Bushell G, Amal R, 2000. Measurement of fractal aggregates of polydisperse particles using small angle light scattering. *Journal of Colloid & Interface Science*, 221(2): 186–194.

Chen Y, Dong B Z, Gao N Y, Fan J C, 2007. Effect of coagulation pretreatment on fouling of an ultrafiltration membrane. *Desalination*, 204(1-3): 181–188.

Cheng W P, 2002. Comparison of hydrolysis/coagulation behavior of polymeric and monomeric iron coagulants in humic acid solution. *Chemosphere*, 47(9): 963–969.

Cheng W P, Chi F H, 2002. A study of coagulation mechanisms of polyferric sulfate reacting with humic acid using a fluorescence-quenching method. *Water Research*, 36(18): 4583–4591.

Choi K Y J, Dempsey B A, 2004. In-line coagulation with low-pressure membrane filtration. *Water Research*, 38(19): 4271–4278.

Duan J M, Gregory J, 2003. Coagulation by hydrolysing metal salts. *Advances in Colloid & Interface Science*, 100-102: 475–502.

Guigui C, Rouch J C, Durand-Bourlier L, Bonnelye V, Aptel P, 2002. Impact of coagulation conditions on the in-line coagulation/UF process for drinking water production. *Desalination*, 147(1-3): 95–100.

Howe K J, Clark M M, 2006. Effect of coagulation pretreatment on membrane filtration performance. *Journal of American Water Works Association*, 98(4): 133–139.

Howe K J, Marwah A, Chiu K P, Adham S S, 2006. Effect of coagulation on the size of MF and UF membrane foulants. *Environmental Science & Technology*, 40(24): 7908–7913.

Huang C P, Lin J L, Lee W S, Pan J R, Zhao B Q, 2011. Effect of coagulation mechanism on membrane permeability in coagulation-assisted microfiltration for spent filter backwash water recycling. *Colloids and Surfaces A: Physicochemical and Engineering Aspects*, 378(1-3): 72–78.

Kimura K, Maeda T, Yamamura H, Watanabe Y, 2008. Irreversible membrane fouling in microfiltration membranes filtering coagulated surface water. *Journal of Membrane Science*, 320(1-2): 356–362.

Lee S Y A, Fane A G, Waite T D, 2005. Impact of natural organic matter on floc size and structure effects in membrane filtration. *Environmental Science & Technology*, 39(17): 6477–6486.

Lee J D, Lee S H, Jo M H, Park P K, Lee C H, Kwak J W, 2000. Effect of coagulation conditions on membrane filtration characteristics in coagulation-microfiltration process for water treatment. *Environmental Science & Technology*, 34(17): 3780–3788.

Lei G Y, Ma J, Guan X H, Song A K, Cui Y J, 2009. Effect of basicity on coagulation performance of polyferric chloride applied in eutrophicated raw water. *Desalination*, 247(1-3): 518–529.

Lin J L, Huang C P, Pan J R, Wang D S, 2008. Effect of Al(III) speciation on coagulation of highly turbid water. *Chemosphere*, 72(2): 189–196.

Liu T K, Chin C J M, 2009. Improved coagulation performance using preformed polymeric iron chloride (PICl). *Colloids and Surfaces A*: *Physicochemical and Engineering Aspects*, 339(1-3): 192–198.

Park P K, Lee C H, Choi S J, Choo K H, Kim S H, Yoon C H et al., 2002. Effect of the removal of DOMs on the performance of a coagulation-UF membrane system for drinking water production. *Desalination*, 145(1-3): 237–245.

Thurman E M, Malcolm R L, 1981. Preparative isolation of aquatic humic substances. *Environmental Science & Technology*, 15(4): 463–466.

Waite T D, 1999. Measurement and implications of floc structure in water and wastewater treatment. *Colloids and Surfaces A: Physicochemical and Engeering Aspects*, 151(1-2): 27–41.

Wang J, Guan J, Santiwong S R, David T D, 2008. Characterization of floc size and structure under different monomer and polymer coagulants on microfiltration membrane fouling. *Journal of Membrane Science*, 321(2): 132–138.

Wang J, Guan J, Santiwong S R, David T D, 2010. Effect of aggregate characteristics under different coagulation mechanisms on microfiltration membrane fouling. *Desalination*, 258(1-3): 19–27.

JOURNAL OF ENVIRONMENTAL SCIENCES

(http://www.jesc.ac.cn)

Aims and scope

Journal of Environmental Sciences is an international academic journal supervised by Research Center for Eco-Environmental Sciences, Chinese Academy of Sciences. The journal publishes original, peer-reviewed innovative research and valuable findings in environmental sciences. The types of articles published are research article, critical review, rapid communications, and special issues.

The scope of the journal embraces the treatment processes for natural groundwater, municipal, agricultural and industrial water and wastewaters; physical and chemical methods for limitation of pollutants emission into the atmospheric environment; chemical and biological and phytoremediation of contaminated soil; fate and transport of pollutants in environments; toxicological effects of terrorist chemical release on the natural environment and human health; development of environmental catalysts and materials.

For subscription to electronic edition

Elsevier is responsible for subscription of the journal. Please subscribe to the journal via http://www.elsevier.com/locate/jes.

For subscription to print edition

China: Please contact the customer service, Science Press, 16 Donghuangchenggen North Street, Beijing 100717, China. Tel: +86-10-64017032; E-mail: journal@mail.sciencep.com, or the local post office throughout China (domestic postcode: 2-580).

Outside China: Please order the journal from the Elsevier Customer Service Department at the Regional Sales Office nearest you.

Submission declaration

Submission of an article implies that the work described has not been published previously (except in the form of an abstract or as part of a published lecture or academic thesis), that it is not under consideration for publication elsewhere. The submission should be approved by all authors and tacitly or explicitly by the responsible authorities where the work was carried out. If the manuscript accepted, it will not be published elsewhere in the same form, in English or in any other language, including electronically without the written consent of the copyright-holder.

Submission declaration

Submission of the work described has not been published previously (except in the form of an abstract or as part of a published lecture or academic thesis), that it is not under consideration for publication elsewhere. The publication should be approved by all authors and tacitly or explicitly by the responsible authorities where the work was carried out. If the manuscript accepted, it will not be published elsewhere in the same form, in English or in any other language, including electronically without the written consent of the copyright-holder.

Editorial

Authors should submit manuscript online at http://www.jesc.ac.cn. In case of queries, please contact editorial office, Tel: +86-10-62920553, E-mail: jesc@263.net, jesc@rcees.ac.cn. Instruction to authors is available at http://www.jesc.ac.cn.

Journal of Environmental Sciences (Established in 1989)
Vol. 25 No. 2 2013

Supervised by	Chinese Academy of Sciences	**Published by**	Science Press, Beijing, China
Sponsored by	Research Center for Eco-Environmental		Elsevier Limited, The Netherlands
	Sciences, Chinese Academy of Sciences	**Distributed by**	
Edited by	Editorial Office of Journal of	Domestic	Science Press, 16 Donghuangchenggen
	Environmental Sciences		North Street, Beijing 100717, China
	P. O. Box 2871, Beijing 100085, China		Local Post Offices through China
	Tel: 86-10-62920553; http://www.jesc.ac.cn	Foreign	Elsevier Limited
	E-mail: jesc@263.net, jesc@rcees.ac.cn		http://www.elsevier.com/locate/jes
Editor-in-chief	Hongxiao Tang	**Printed by**	Beijing Beilin Printing House, 100083, China

CN 11-2629/X **Domestic postcode: 2-580** **Domestic price per issue RMB ¥ 110.00**

ISSN 1001-0742